Inorg. Chem. **2004**, *43*, 1159–1166

Synthesis and Characterization of Binucleating Bis(amidinate) Ligands and Their Dialuminum Complexes

Bronya Clare, Niladri Sarker, Richard Shoemaker, and John R. Hagadorn*

Department of Chemistry and Biochemistry, University of Colorado, Boulder, Colorado 80309-0215

Received September 3, 2003

Two general routes to binucleating bis(amidinate) ligands based on dibenzofuran and 9,9-dimethylxanthene backbones are reported. The free-base form of one of the ligands, $^{Ph,Mes}L_{DBF}H_2$, forms a 1:1 adduct with acetone. Single-crystal X-ray diffraction of this adduct reveals bidentate H-bonding of the bis(amidine) to the ketone oxygen. Bond lengths suggest that the individual H-bonds are relatively weak, yet IR spectroscopy shows a significant –26 cm^{-1} shift for the carbonyl stretch relative to free acetone. Additionally, the new dialuminum complexes $^{iPr}L_{DBF}Al_2Me_4$ (**3**), $^{iPr}L_{Xan}Al_2Me_4$ (**4**), $^{tBu,Et}L_{DBF}Al_2Me_4$ (**5**), and $^{tBu,Et}L_{Xan}Al_2Me_4$ (**6**) are prepared by reaction of Al_2Me_6 with the bis(amidines) in toluene solution. ^1H NMR spectroscopic studies indicate that **3** and **4** interact weakly with certain Lewis bases (DMSO, DMF, pyridine) to effect the exchange of the Al-bound Me groups. Other bases, such as THF and TMEDA, fail to interact. Solid-state structures for **3** and **4** are reported.

Introduction

Dialuminum complexes are increasingly being used as catalysts (and cocatalysts) in a range of small-molecule transformations including carbonyl additions[1−6] and olefin polymerizations.[7−10] Much of the interest in these complexes is due to their potential to access cooperative bimetallic mechanisms that are not possible for mononuclear systems.[11]

Scheme 1

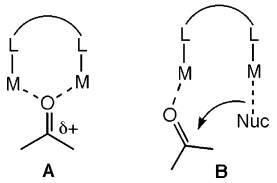

For example, in carbonyl activations using dinuclear Lewis acids, one mechanistic pathway that is often proposed involves the formation of bridged adduct **A** (Scheme 1), which features a highly electrophilic carbonyl carbon by virtue of "double activation" by coordination to a pair of electron-deficient metals.[12,13] Alternatively, bimetallics are often thought to function as ambifunctional catalysts (**B**),[14,15] with one metal providing a Lewis acidic site and the other providing a nucleophile for simultaneous carbonyl activation and attack.

Direct structural and spectroscopic evidence supporting the above mechanisms in dialuminum complexes is rare. Indeed, for many catalytic systems the presence of a dinuclear cooperative mechanism is inferred largely by reactivity comparisons to related mononuclear species.

* Author to whom correspondence should be addressed. E-mail: john.hagadorn@colorado.edu.

(1) Ooi, T.; Takahashi, M.; Maruoka, K. *J. Am. Chem. Soc.* **1996**, *118*, 11307−11308.
(2) Ooi, T.; Tayama, E.; Takahashi, M.; Maruoka, K. *Tetrahedron Lett.* **1997**, *38*, 7403−7406.
(3) Ooi, T.; Takahashi, M.; Maruoka, K. *Angew. Chem., Int. Ed.* **1998**, *37*, 835−837.
(4) Hanawa, H.; Maekawara, N.; Maruoka, K. *Tetrahedron Lett.* **1999**, *40*, 8379−8382.
(5) Ooi, T.; Itagaki, Y.; Miura, T.; Maruoka, K. *Tetrahedron Lett.* **1999**, *40*, 2137−2138.
(6) Ooi, T.; Miura, T.; Takaya, K.; Maruoka, K. *Tetrahedron Lett.* **1999**, *40*, 7695−7698.
(7) Eisch, J. J.; Otieno, P. O.; Mackenzie, K.; Kotowicz, B. W. *ACS Symp. Ser.* **2002**, *822*, 88−103.
(8) Budzelaar, P. H. M.; Talarico, G. *ACS Symp. Ser.* **2002**, *822*, 142−152.
(9) Piers, W. E.; Irvine, G. J.; Williams, V. C. *Eur. J. Inorg. Chem.* **2000**, 2131−2142.
(10) Chen, E. Y. X.; Marks, T. J. *Chem. Rev.* **2000**, *100*, 1391−1434.
(11) For selected reviews and articles on dinuclear catalysts in organic synthesis, see: (a) Steinhagen, H.; Helmchen, G. *Angew. Chem., Int. Ed.* **1996**, *35*, 2339−2342. (b) Shibasaki, M.; Sasai, H.; Arai, T. *Angew. Chem., Int. Ed.* **1997**, *36*, 1237−1256. (c) Maruoka, K. *Catal. Today* **2001**, *66*, 33−45. (d) Trost, B. M.; Ito, H. *J. Am. Chem. Soc.* **2000**, *122*, 12003−12004.
(12) Wuest, J. D. *Acc. Chem. Res.* **1999**, *32*, 81−89.
(13) Otera, J. In *Carbonyl-Lewis acid complexes*; Wiley-VCH: Weinheim, 2000; pp 1−32.
(14) Rowlands, G. J. *Tetrahedron* **2001**, *57*, 1865−1882.
(15) Williams, N. H.; Takasaki, B.; Wall, M.; Chin, J. *Acc. Chem. Res.* **1999**, *32*, 485−493.

10.1021/ic035035p CCC: $27.50
Published on Web 01/03/2004

Scheme 2

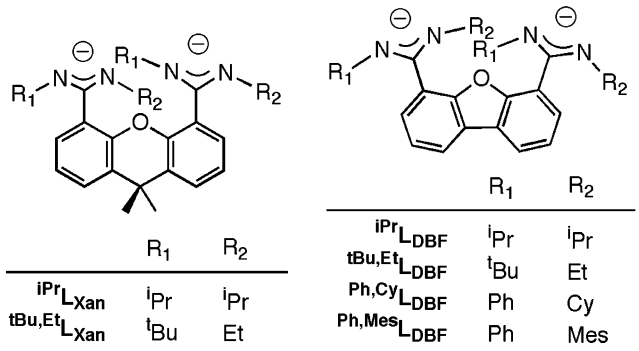

	R_1	R_2
$^{iPr}L_{Xan}$	^{i}Pr	^{i}Pr
$^{tBu,Et}L_{Xan}$	^{t}Bu	Et

	R_1	R_2
$^{iPr}L_{DBF}$	^{i}Pr	^{i}Pr
$^{tBu,Et}L_{DBF}$	^{t}Bu	Et
$^{Ph,Cy}L_{DBF}$	Ph	Cy
$^{Ph,Mes}L_{DBF}$	Ph	Mes

However, a number of well-defined dialuminum systems have demonstrated the viability of bridged adducts related to **A**. Notably, Wuest has reported the only structurally characterized example of a dialuminum μ-carbonyl complex, prepared using an intramolecularly bonded ketone.[16] Related work with stronger Lewis bases has yielded several isolable adducts. Scott recently demonstrated the formation of a complex with an $[Al_2(\mu\text{-Cl})]^{5+}$ core by the addition of external Cl^- to a discrete dialuminum tetraphenolate.[17] Additionally, Uhl has structurally characterized a broad range of base adducts (e.g., N_3^-, RCO_2^-, NO_3^{2-}) of the novel methylene-bridged dialuminum Lewis acid $R_2AlCH_2AlR_2$ ($R = CH(SiMe_3)_2$).[18,19]

We are interested in performing detailed structural and spectroscopic studies on dialuminum complexes to evaluate some of the fundamental properties of Lewis acidic bimetallics and their interactions with Lewis bases. Essential to this work is the use of binucleating ligands to prepare discrete dinuclear complexes. For this, we have been using preorganized bis(amidinates) that allow access to a wide range of bimetallics with control over key structural features, such as intermetal separation and sterics. Here we report the preparation and characterization of several new bis(amidinate) ligands and their dialuminum complexes. Preliminary studies on the coordination of Lewis bases to the dialuminum complexes, which were monitored by solution NMR spectroscopic studies, are also reported. Portions of the bis(amidine) syntheses have been previously communicated.[20,21]

Results and Discussion

Bis(amidinate) Ligands. Shown in Scheme 2 are examples of binucleating bis(amidinate)[22] ligands that we have developed around rigid dibenzofuran and 9,9-dimethylxanthene spacer units. Two general methods have proven useful for their preparation. The first involves the direct reaction of carbodiimides with the dilithiated backbones. For example,

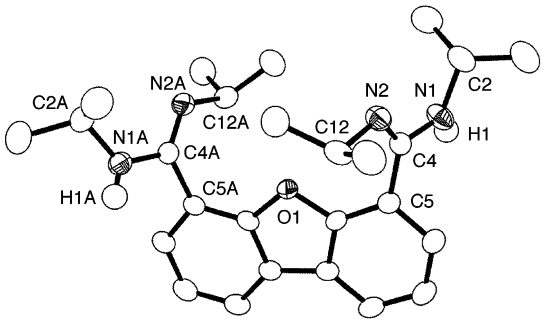

Figure 1. Molecular structure of $^{iPr}L_{DBF}H_2$ drawn with 50% thermal ellipsoids.

4,6-dilithiodibenzofuran was formed by the reaction of dibenzofuran with 2.4 equiv of BuLi-TMEDA as described by Haenel and co-workers.[23] The addition of 1,3-diisopropylcarbodiimide to this mixture, followed by aqueous workup and crystallization from CH_3CN, afforded bis(amidine) $^{iPr}L_{DBF}H_2$ in 67% yield. By this simple procedure a range of symmetric and unsymmetric bis(amidines) can be prepared by variation of the carbodiimide. The bis(amidines) display many desirable properties from a synthetic standpoint. They can be conveniently prepared in up to 50 g quantities and purified by crystallization from hydrocarbons or CH_3CN. ^1H NMR spectroscopic data for the bis(amidines) is often complex due to the presence of interconverting solution structures. However, the spectra are highly solvent dependent, and while the ^1H NMR spectrum of a $CDCl_3$ solution of $^{iPr}L_{DBF}H_2$ is complex, the same compound in D_6-acetone displays the expected number of resonances for a highly symmetric structure indicating fast proton hopping between the "amine" (N−H) and "imine" (C═N) positions of the amidines. IR spectroscopic data of $^{iPr}L_{DBF}H_2$ (mineral oil mull) shows the expected absorptions at 3436 and 1644 cm^{-1} due to the amidine υ_{NH} and $\upsilon_{N=C}$ modes. The solid-state structure of $^{iPr}L_{DBF}H_2$ is shown in Figure 1. The bis(amidine) molecule is located on a crystallographic C_2-axis which passes through the dibenzofuran oxygen. Each amidine adopts an *E*,trans configuration. The high quality of the data allowed for the location and subsequent refinement of the amidine hydrogen (H1). Analysis of bond lengths reveals features typical of amidines. The N1−C4 distance of 1.382(3) Å is ca. 0.09 Å shorter than a true C−N single bond, indicating significant π-interaction similar to that found in amides ($C-N_{ave}$, 1.322). The N2−C4 distance of 1.280(3)

(16) Sharma, V.; Simard, M.; Wuest, J. D. *J. Am. Chem. Soc.* **1992**, *114*, 7931−7933.
(17) Cottone III, A.; Scott, M. J. *Organometallics* **2000**, *19*, 5254−5256.
(18) Uhl, W.; Hannemann, F. *J. Organomet. Chem.* **1999**, *579*, 18−23.
(19) Uhl, W.; Hannemann, F.; Saak, W.; Wartchow, R. *Eur. J. Inorg. Chem.* **1998**, 921−926.
(20) Hagadorn, J. R. *Chem. Commun.* **2001**, 2144−2145.
(21) Hagadorn, J. R.; McNevin, M. J. *Organometallics* **2003**, *22*, 609−611.
(22) For other reported bis(amidinates), see: (a) Appel, S.; Weller, F.; Dehnicke, K. *Z. Anorg. Allg. Chem.* **1990**, *583*, 7−16. (b) Hagadorn, J. R.; Arnold, J. *Angew. Chem., Int. Ed.* **1998**, *37*, 1729−1731. (c) Babcock, J. R.; Incarvito, C.; Rheingold, A. L.; Fettinger, J. C.; Sita, L. R. *Organometallics* **1999**, *18*, 5729−5732. (d) Chen, C. T.; Rees, L. H.; Cowley, A. R.; Green, M. L. H. *J. Chem. Soc., Dalton Trans.* **2001**, 1761−1767. (e) Bambirra, S.; Meetsma, A.; Hessen, B.; Teuben, J. H. *Organometallics* **2001**, *20*, 782−785. (f) Walther, D.; Stollenz, M.; Bottcher, L.; Gorls, H. *Z. Anorg. Allg. Chem.* **2001**, *627*, 1560−1570. (g) Kawaguchi, H.; Matsuo, T. *Chem. Commun.* **2002**, 958−959. (h) Li, J.-F.; Weng, L.-H.; Wei, X.-H.; Liu, D.-S. *J. Chem. Soc., Dalton Trans.* **2002**, 1401−1405. (i) Grundy, J.; Coles, M. P.; Hitchcock, P. B. *J. Organomet. Chem.* **2002**, *662*, 178−187. (j) Chen, C.-T.; Huang, C.-A.; Tzeng, Y.-R.; Huang, B.-H. *J. Chem. Soc., Dalton Trans.* **2003**, 2585−2590.
(23) Haenel, M. W.; Jakubik, D.; Rothenberger, E.; Schroth, G. *Chem. Ber.* **1991**, *124*, 1705−1710.

Scheme 3

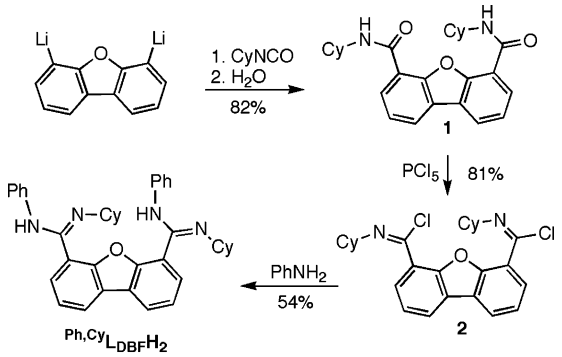

Å) shows a slight elongation (ca. 0.01 Å) relative to isolated C−N double bonds.

A second useful approach for the synthesis of bis(amidines) involves the initial preparation of dibenzofuran-bridged bis(amides), followed by their conversion to bis(amidines). An example of this method is shown in Scheme 3. Reaction of 4,6-dilithiodibenzofuran with cyclohexylisocyanate afforded bis(amide) **1** in high yield. Conversion of **1** to bis(imidoyl chloride) **2** was achieved by treatment with PCl_5 in CH_2Cl_2. **2** was converted to the unsymmetric bis(amidine) $^{Ph,Cy}L_{DBF}H_2$ in moderate yield by reaction with 4 equiv of $PhNH_2$. Using the same methodology, $^{Ph,Mes}L_{DBF}H_2$ was synthesized in moderate yield from 4,6-dilithiodibenzofuran, phenylisocyanate, and 2,4,6-trimethylaniline. Crystallization of this bis(amidine) from hydrocarbon solvents proved difficult until a trace amount of acetone was added, upon which yellow crystals of the adduct $^{Ph,Mes}L_{DBF}H_2$·acetone formed. The IR spectrum of $^{Ph,Mes}L_{DBF}H_2$·acetone (KBr pellet) revealed the carbonyl stretch of the H-bonded acetone at 1694 cm^{-1}, which is significantly red shifted compared to that of free acetone at 1720 cm^{-1}. Shifts of similar magnitude have been reported for carbonyl adducts to bis(phenols) which feature a pair of H-bonds to the oxygen atom.[24−26]

The solid-state structure of $^{Ph,Mes}L_{DBF}H_2$·acetone is shown in Figure 2. Noticeably, the pair of amidine N−H functionalities are H-bonded to a single acetone molecule, giving a 1:1 adduct of approximate C_s symmetry. The acetone lone pairs are directed toward the amidine N−H groups. Thus, the plane defined by O2−C45−C46−C47 intersects that defined by N2−O2−N3 at an angle of only 4(1)°. The acetone is symmetrically coordinated with average O−H and O−N distances of 2.18 and 3.01 Å, respectively. These values are significantly longer than those for typical H-bonding interactions. For example, H-bonds between ketones and neutral amines generally feature O−H and O−N distances of 1.97 and 2.85 Å, respectively.[27] Thus, while double H-bonding here is clearly preferred, the formation of the second H-bond apparently leads to the weakening of the *individual* H-bond strengths.

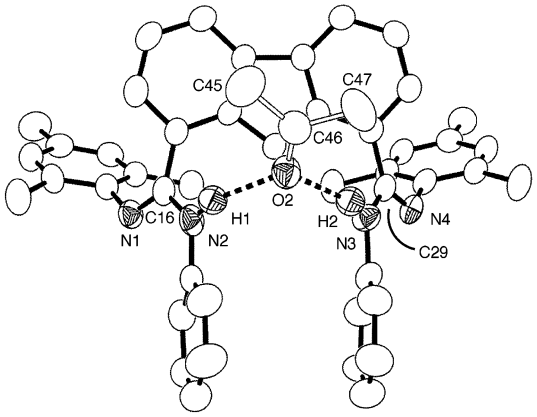

Figure 2. Molecular structure of $^{Ph,Mes}L_{DBF}H_2$·acetone drawn with 50% thermal ellipsoids.

Scheme 4

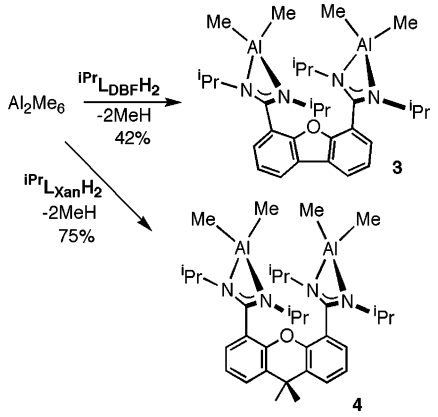

Dialuminum Complexes. The addition of Al_2Me_6 to a toluene solution of $^{i\text{Pr}}L_{DBF}H_2$ led to immediate gas evolution. Following workup in Et_2O solution and cooling to −40 °C, dialuminum complex **3** (Scheme 4) was isolated in 42% yield as colorless crystals. The analogous reaction using the 9,9-dimethylxanthene-bridged ligand, $^{i\text{Pr}}L_{Xan}H_2$, afforded **4** in 75% isolated yield. To demonstrate the structural effects of varying the linker group, single-crystal X-ray diffraction studies were performed on both **3** and **4** (Figure 3). As expected, each of the pseudotetrahedral Al centers of **3** and **4** features a bidentate amidinate (Al−N_{ave}, 1.93 Å) and a pair of Me donors (Al−Me_{ave}, 1.95 Å). Related, mononuclear complexes supported by amidinato,[28−30] triazenido,[31] guanidinato,[32] and other[33−38] ligands feature similar geometries and metrical parameters. While the metal geometries

(24) Saied, O.; Simard, M.; Wuest, J. D. *J. Org. Chem.* **1998**, *63*, 3756−3757.
(25) Hine, J.; Ahn, K. *J. Org. Chem.* **1987**, *52*, 2083−2086.
(26) Hine, J.; Linden, S. M.; Kanagasabapathy, V. M. *J. Org. Chem.* **1985**, *50*, 5096−5099.
(27) Taylor, R.; Kennard, O. *Acc. Chem. Res.* **1984**, *17*, 320−326.
(28) Schmidt, J. A. R.; Arnold, J. *Organometallics* **2002**, *21*, 2306−2313.
(29) Coles, M. P.; Swenson, D. C.; Jordan, R. F.; Young, V. G., Jr. *Organometallics* **1997**, *16*, 5183−5194.
(30) Dagorne, S.; Guzei, I. A.; Coles, M. P.; Jordan, R. F. *J. Am. Chem. Soc.* **2000**, *122*, 274−289.
(31) Leman, J. T.; Braddock-Wilking, J.; Coolong, A. J.; Barron, A. R. *Inorg. Chem.* **1993**, *32*, 4324−4336.
(32) Aeilts, S. L.; Coles, M. P.; Swenson, D. C.; Jordan, R. F.; Young, V. G., Jr. *Organometallics* **1998**, *17*, 3265−3270.
(33) Coles, M. P.; Swenson, D. C.; Jordan, R. F.; Young, V. G., Jr. *Organometallics* **1998**, *17*, 4042−4048.
(34) Qian, B.; Ward, D. L.; Smith III, M. R. *Organometallics* **1998**, *17*, 3070−3076.
(35) Walfort, B.; Leedham, A. P.; Russell, C. A.; Stalke, D. *Inorg. Chem.* **2001**, *40*, 5668−5674.
(36) Dias, H. V. R.; Jin, W.; Ratcliff, R. E. *Inorg. Chem.* **1995**, *34*, 6100−6105.

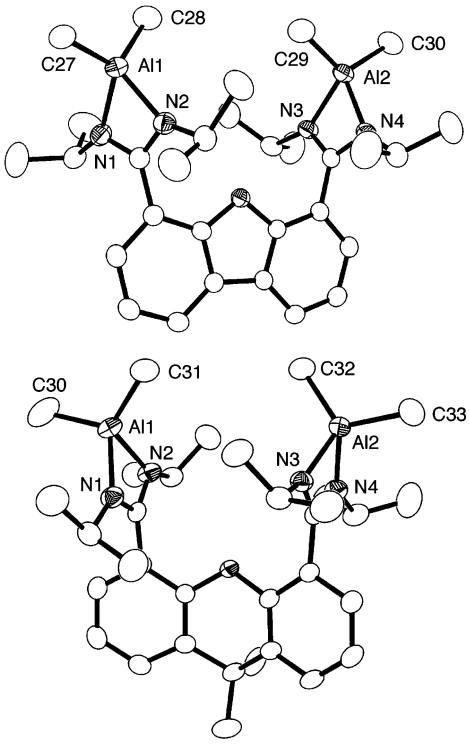

Figure 3. Molecular structures of **3** (top) and **4** (bottom) drawn with 50% thermal ellipsoids.

are similar for **3** and **4**, the differing ligand backbones result in a significant difference in their intermetal separations. Thus, for **3** the Al1−Al2 distance is 6.5050(9) Å while that for **4** is 5.9303(9) Å. This difference of 0.57 Å is less than expected based on simple molecular mechanics calculations (Chem 3D). We attribute this to steric repulsions between C31 and C32 in **4** that force the Al centers out of the $NCN_{amidinate}$ planes by an average of 0.272 Å. For comparison, the Al centers in **3** rest an average of 0.096 Å out of their $NCN_{amidinate}$ planes.

NMR spectroscopic data indicate that the solution structures of **3** and **4** each feature overall C_{2v} symmetry. For example, the ^{1}H NMR spectrum of **3** (in C_6D_6) features a total of eight resonances. This includes six for the bis(amidinate), which features diastereotopic ^{i}Pr methyls, and a pair of upfield resonances for the two inequivalent Al-bound methyls. The Al−Me resonances appear at δ −0.01 and −0.05 ppm as singlets. The ^{1}H NMR spectrum of **4** under identical conditions is very similar to that of **3** although the Al−Me resonances are more separated and appear at δ 0.02 and −0.11 ppm. To determine if the Al−Me groups were undergoing slow exchange, one-dimensional (1D) selective GOESY[39] experiments were performed on **4** (in D_8-toluene) at 20 °C with mixing times of 0.1−2.5 s. The selective GOESY sequence is a 1D analogue to the conventional two-dimensional (2D) EXCHSY/NOESY experiment, commonly used to investigate dynamic exchange processes

Scheme 5

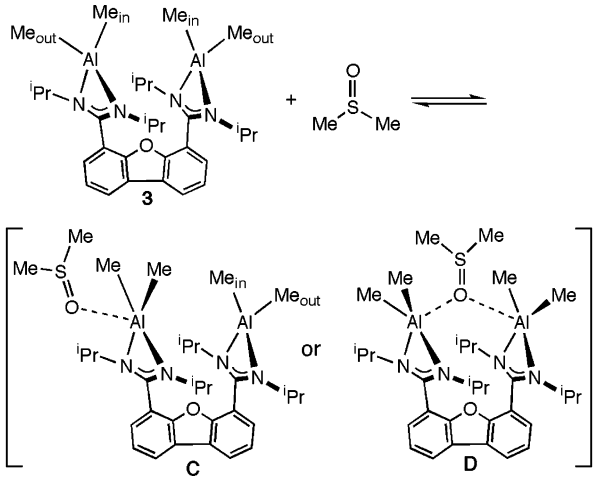

that are slow on the NMR time scale. The selective 1D experiment, however, can be completed in 10 min for all mixing times observed, whereas the full 2D EXCHSY experiment would require hours. Within the limits of T1 (mixing time = 2.5 s), no exchange was observed between the Al−Me groups.

The four-coordinate Al centers of **3** and **4** did not form isolable adducts with a variety of Lewis bases, including THF, dimethyl sulfoxide (DMSO), and pyridine (Py). However, the 20 °C ^{1}H NMR spectrum of **3** in C_6D_6 in the presence of 1 equiv of DMSO revealed a single resonance at δ −0.03 ppm ($\omega_{1/2}$ = 2.5 Hz) for the Al−Me groups, indicating rapid exchange of the "inside" (Me_{in}) and "outside" (Me_{out}) methyls (Scheme 5). Despite the coalescence of the Al−Me groups, none of the bis(amidinate) or DMSO resonances were shifted noticeably. These data are consistent with the transient formation of a thermodynamically disfavored adduct, such as **C** or **D**, leading to the formation of an intermediate in which the two methyls at a single Al center become indistinguishable. Dissociation of the DMSO would lead to the scrambling of Me_{in} and Me_{out}. Repeating the experiment with **3** in the presence of 1 equiv of DMF gave similar coalescence of Me_{in} and Me_{out}, although the resonance was broader ($\omega_{1/2}$ = 9.9 Hz), indicating a less rapid exchange process. Upon cooling of this solution (**3** + DMF), the peak further broadened (T_c = −42(2) °C) and at −79.9 °C two distinct resonances were observed, indicating that exchange was slow at that temperature. 1D GOESY experiments determined that measurable exchange was occurring at 0.1 ms mixing time. Fitting the extent of exchange to a range of mixing times from 0.1 to 2.5 ms gave $\Delta G‡$ = 12.7(6) kcal/mol for the Lewis-base-mediated process.

To further probe the solution dynamics of the dialuminum complexes, the unsymmetrical bis(amidines) $^{tBu,Et}L_{DBF}H_2$ and $^{tBu,Et}L_{Xan}H_2$ were reacted with Al_2Me_6 to prepare **5** and **6**, respectively. ^{1}H NMR spectroscopic analysis of **6** in C_6D_6 revealed it to be a 1:0.9 mixture of C_2-**6** and C_s-**6** (Scheme 6). This ratio did not change over 24 h at room temperature, but heating the solution to 70 °C overnight caused the ratio to change to 1:1. Further heating did not lead to additional change. Thus, the equilibrium for two rotational diastereo-

(37) Schulz, S.; Nieger, M.; Hupfer, H.; Roesky, P. W. *Eur. J. Inorg. Chem.* **2000**, 1623−1626.
(38) Radzewich, C. E.; Coles, M. P.; Jordan, R. F. *J. Am. Chem. Soc.* **1998**, *120*, 9384−9385.
(39) Stonehouse, J.; Adell, P.; Keeler, J.; Shaka, A. J. *J. Am. Chem. Soc.* **1994**, *116*, 6037−6038.

Scheme 6

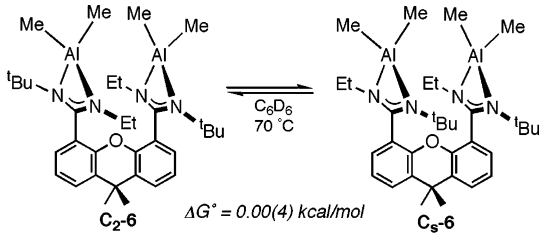

mers is thermoneutral ($\Delta G^\circ = 0.00(4)$ kcal/mol). Similar studies with compound **5** gave $\Delta G^\circ = 0.10(4)$ kcal/mol, although it remains unknown which diastereomer is favored.

In summary, we have reported the synthesis of several new binucleating bis(amidinate) ligands supported by rigid dibenzofuran and 9,9-dimethylxanthene spacers. These ligands were used for the preparation of structurally characterized dialuminum complexes which were shown to interact weakly with a variety of Lewis bases in solution to effect Me group exchange. Reactivity studies of these complexes and related bimetallic Lewis acids are ongoing.

Experimental Section

General Considerations. Standard Schlenk line and glovebox techniques were used unless stated otherwise. 2,4,6-Trimethylaniline ($MesNH_2$), 1,3-diisopropylcarbodiimide, 1-*tert*-butyl-3-ethylcarbodiimide, cyclohexylisocyanate (CyNCO), and phenylisocyanate (PhNCO) were purchased from Aldrich and sparged with N_2 prior to use. *n*-Butyllithium (BuLi) solutions were purchased from Alfa and were used as received. Dibenzofuran was sublimed at 50 mTorr/70 °C prior to use. *N*,*N*,*N*′,*N*′-Tetramethylethylenediamine (TMEDA) was distilled from Na under nitrogen. Aniline, *N*,*N*-dimethylformamide (DMF), dimethyl sulfoxide (DMSO), and pyridine (Py) were distilled from CaH_2 under N_2. Hexanes, Et_2O, toluene, tetrahydrofuran (THF), and CH_2Cl_2 were passed through columns of activated alumina and sparged with N_2 prior to use. D_6-Benzene and D_8-toluene were vacuum transferred from Na/benzophenone ketyl. $CDCl_3$ and D_6-acetone were vacuum transferred from CaH_2. Chemical shifts (δ) for ^{1}H NMR spectra are given relative to residual protium in the deuterated solvent at δ 7.15, 7.27, 2.10, and 2.04 ppm for C_6D_6, $CDCl_3$, D_8-toluene, and D_6-acetone, respectively. Samples were prepared as KBr pellets for infrared absorption spectroscopy unless stated otherwise. Elemental analyses were determined by Desert Analytics. For each series of closely related compounds at least one representative was submitted for elemental analysis.

Preparation of Bis(amidines). Two general methods were used for the preparation of the bis(amidines) shown in Scheme 1. Method A was used for the preparation of $^{i\mathrm{Pr}}L_{\mathrm{Xan}}H_2$, $^{t\mathrm{Bu,Et}}L_{\mathrm{Xan}}H_2$, $^{i\mathrm{Pr}}L_{\mathrm{DBF}}H_2$, and $^{t\mathrm{Bu,Et}}L_{\mathrm{DBF}}H_2$. Method B was used for the preparation of $^{\mathrm{Ph,Cy}}L_{\mathrm{DBF}}H_2$ and $^{\mathrm{Ph,Mes}}L_{\mathrm{DBF}}H_2$. Representative procedures are given below for each method. ^{1}H and ^{13}C{^{1}H} NMR spectroscopic data are given whenever possible. However, often the bis(amidines) displayed complex and broad spectra due to the presence of numerous interconverting structures in solution.

Method A: Preparation of $^{i\mathrm{Pr}}L_{\mathrm{DBF}}H_2$. Dibenzofuran (30.8 g, 183 mmol), TMEDA (66.7 mL, 439 mmol), and hexanes (500 mL) were combined in a 2-L round-bottomed flask equipped with an addition funnel and a reflux condenser. A hexanes solution of BuLi (157 mL, 439 mmol) was added to the clear colorless solution over 45 min. The resulting yellow suspension was heated to reflux for 1 h. Upon heating, gas evolution was observed. At ambient temperature, diisopropylcarbodiimide (55.4 g, 439 mmol) was added dropwise over 45 min to form a bright yellow suspension. After stirring overnight, H_2O (400 mL) was added to the suspension to form a colorless suspension which was stirred for 30 min. The solid was collected on a fritted disk, washed thoroughly with water, and dried in air. ^{1}H NMR spectroscopic analysis of this crude product showed it to be $^{i\mathrm{Pr}}L_{\mathrm{DBF}}H_2$·TMEDA. Heating the solid to 90 °C at 50 mTorr yielded the TMEDA-free product which was purified by recrystallization from hot toluene (52.0 g, 67.6%). ^{1}H NMR (C_6D_6): δ 7.62 (d, $J = 7.5$ Hz, 2H), 7.24 (d, $J = 7.5$ Hz, 2H), 7.08 (t, $J = 7.5$ Hz, 2H), 4.49 (br s, 2H, NC*H*Me$_2$), 3.42 (br s, 2H, NC*H*Me$_2$), 3.37 (br s, 2H, N*H*), 1.31 (br s, 12H, NCH*Me*$_2$), 1.16 (br s, 12H, NCH*Me*$_2$) ppm. ^{13}C{^{1}H} NMR (C_6D_6): δ 153.5, 150.6, 127.7, 125.0, 123.6, 122.4, 121.3, 51.7 (br), 42.9 (br), 26.3 (br), 23.3 (br) ppm. IR: 3434 (s), 3428 (s), 3255 (w), 3055 (w), 3042 (w), 3022 (w), 2964 (s), 2953 (s), 2934 (m), 2913 (m), 2897 (m), 2861 (m), 2609 (w), 2375 (w), 2347 (w), 1696 (w), 1685 (w), 1676 (w), 1633 (s), 1605 (m), 1577 (w), 1571 (w), 1566 (w), 1560 (w), 1550 (w), 1541 (w), 1534 (w), 1488 (s), 1468 (s), 1449 (s), 1426 (s), 1406 (m), 1381 (w), 1375 (w), 1356 (m), 1316 (m), 1272 (m), 1233 (w), 1190 (s), 1172 (s), 1125 (m), 1110 (w), 1059 (w), 1013 (w), 977 (w), 972 (w), 959 (w), 938 (w), 921 (w), 905 (w), 883 (w), 870 (w), 860 (w), 847 (w), 809 (w), 719 (s), 754 (m), 703 (w), 664 (w), 638 (w), 603 (w), 574 (w), 561 (w), 503 (w), 477 (w), 470 (w), 455 (w), 421 (w) cm^{-1}. Anal. Calcd (found) for $^{i\mathrm{Pr}}L_{\mathrm{DBF}}H_2$·0.75(toluene), $C_{31.25}H_{42}N_4O$: C, 76.65 (76.60); H, 8.64 (8.55); N, 11.44 (11.45).

Method B: Preparation of $^{\mathrm{Ph,Cy}}L_{\mathrm{DBF}}H_2$. Hexanes (350 mL) and TMEDA (53.0 mL, 349 mmol) were added to dibenzofuran (24.5 g, 145 mmol) to form a clear, pale yellow solution. A hexanes solution of BuLi (125 mL, 349 mmol) was added dropwise over 45 min. The resulting yellow suspension was heated to reflux for 1 h. The solution was cooled to 0 °C and CyNCO (44.3 g, 349 mmol) was added over 10 min to form an orange suspension. After stirring overnight, H_2O (500 mL) was added to the suspension. The resulting orange solid was collected on a fritted disk and thoroughly washed with 1 M HCl (400 mL) and water until the water washes were no longer basic. The solid was then dried by azeotropic distillation with benzene (500 mL) using a Dean−Stark trap. The bis(amide) derivative **1** (Scheme 2) was isolated as a white solid, washed with hexanes (2 × 200 mL), and dried under reduced pressure (49.8 g, 82.1%). ^{1}H NMR ($CDCl_3$): δ 8.02 (d, $J = 8.0$ Hz, 2H), 8.01 (d, $J = 7.5$ Hz, 2H), 7.43 (t, $J = 7.8$ Hz, 2H), 6.90 (d, $J = 7.5$ Hz, 2H, N*H*), 4.09 (m, 2H, α-Cy*H*), 1.10−2.20 (20H, Cy-*H*) ppm. ^{13}C{^{1}H} NMR ($CDCl_3$): δ 163.5, 152.8, 128.5, 124.5 123.9, 123.7, 119.9, 49.4, 33.4, 25.8, 25.2 ppm. CH_2Cl_2 (800 mL) and PCl_5 (27.1 g, 130 mmol) were heated to reflux for 25 min to form a clear colorless solution. At ambient temperature, a portion of **1** (27.2 g, 65.0 mmol) was added and the resulting suspension was heated to reflux under N_2. Within 2 h a clear yellow solution had formed. After 24 h, the volatiles were removed under reduced pressure and the resulting yellow solid was washed with hexanes to afford **2** (24 g, 81%). ^{1}H NMR ($CDCl_3$): δ 7.98 (d, $J = 7.6$ Hz, 2H), 7.90 (d, $J = 7.6$ Hz, 2H), 7.38 (t, $J = 7.6$ Hz, 2H), 4.02 (m, 2H, α-Cy*H*), 1.32−2.01 (20H, Cy*H*) ppm. ^{13}C{^{1}H} NMR (C_6D_6): δ 154.2, 134.7, 129.4, 125.5, 123.3, 123.2, 123.1, 63.5, 33.4, 26.4, 24.9 ppm. Aniline (8.0 mL, 88.0 mmol) was added dropwise over 2 min to a CH_2Cl_2 (120 mL) solution of **2** (10.0 g, 22.0 mmol). The resulting orange solution was stirred overnight. H_2O (500 mL) was added to form a biphasic suspension, to which dilute HCl was added (pH 1). To the separated organic layer, 1 M NaOH (450 mL) was added and the biphasic suspension was stirred for 2 h. The organics were separated, dried over $MgSO_4$, and filtered.

Removal of volatiles under reduced pressure afforded crude product, which was crystallized from CH_2Cl_2 (200 mL) and hexanes (200 mL) at −40 °C to give a white crystalline solid (6.7 g, 54%). ^{1}H NMR (D_6-acetone): δ 7.89 (d, J = 6.8 Hz, 2H), 7.25 (d, J = 6.8 Hz, 2H), 7.18 (t, J = 7.6 Hz, 2H), 6.87 (t, J = 7.2 Hz, 4H), 6.66 (d, J = 7.2 Hz, 4H), 6.59 (t, J = 6.8 Hz, 2H), 6.05 (br, 2H, α-Cy-*H*), 4.19 (br, 2H, N*H*), 2.36−1.28 (20H, Cy-*H*) ppm. ^{13}C{^{1}H} NMR (C_6D_6): δ 153.6, 152.3, 152.0, 129.0, 128.9, 124.9, 123.3, 122.0, 121.8, 50.7, 33.9, 26.6, 25.8 ppm. Two resonances in the ^{13}C{^{1}H} NMR are likely obscured by the solvent. IR: 3451 (m), 3405 (m), 3251 (m, br), 3073 (m), 3048 (m), 3026 (m), 3012 (m), 2927 (s), 2851 (s), 1613 (s), 1591 (s), 1518 (s), 1486 (s), 1460 (m), 1449 (s), 1422 (s), 1405 (s), 1333 (m), 1269 (m), 1256 (s), 1223 (w), 1184 (s), 1169 (s), 1150 (s), 1117 (m), 1088 (w), 1071 (m), 1057 (m), 1024 (w), 998 (w), 976 (w), 958 (w), 923 (w), 905 (w), 892 (m), 872 (w), 852 (m), 801 (w), 784 (s), 761 (s), 747 (s), 694 (s), 648 (w), 635 (w), 578 (w), 566 (w), 556 (w), 550 (w), 505 (w), 464 (w), 446 (w), 414 (s) cm^{-1}. Anal. Calcd (found) for $C_{38}H_{40}N_4O$: C, 80.25 (79.68); H, 7.09 (7.17); N, 9.85 (10.00).

$^{t\text{Bu,Et}}$L$_{\text{DBF}}$H$_2$ was prepared from dibenzofuran and 1-*tert*-butyl-3-ethylcarbodiimide by method A in 35% yield. ^{1}H NMR (C_6D_6): δ 7.59 (d, J = 7.5 Hz, 2H), 7.20 (d, J = 7.5 Hz, 2H), 7.06 (t, J = 7.5 Hz, 2H), 3.60 (s, 2H, N*H*), 3.27 (q, 7.0 Hz, 4H, NCH_2CH$_3$), 1.57 (s, 18H, NCMe_3), 1.30 (t, J = 7.0 Hz, 6H, NCH$_2$CH_3) ppm. ^{13}C{^{1}H} NMR (C_6D_6): δ 153.4, 151.8, 127.5, 125.0, 123.6, 122.3, 121.3, 52.3, 46.6, 29.6, 18.4 ppm. IR: 3439 (s), 3276 (w), 3058 (m), 3029 (m), 2958 (s), 2912 (s), 2877 (s), 2841 (s), 2668 (w), 1943 (w), 1918 (w), 1859 (w), 1800 (w), 1641 (s, br), 1501 (s), 1493 (s), 1445 (s), 1422 (s), 1404 (s), 1388 (s), 1362 (s), 1310 (s), 1292 (s), 1226 (s), 1188 (s), 1162 (m), 1137 (m), 1099 (m), 1061 (s), 1033 (m), 975 (m), 960 (w), 940 (w), 922 (w), 880 (m), 858 (s), 788 (s), 755 (s), 749 (s), 709 (m), 668 (m), 618 (w), 596 (w), 573 (m), 565 (w), 551 (w), 474 (w), 457 (w), 435 (w) cm^{-1}.

$^{\text{Ph,Mes}}$L$_{\text{DBF}}$H$_2$ was prepared from dibenzofuran, PhNCO, and $MesNH_2$ by method B with an overall yield of 12%. Acceptable NMR data could not be obtained due to the interconversion of multiple isomers and/or aggregates on an intermediate time scale. IR: 3362 (s, br), 3057 (m), 2999 (m), 2913 (s), 2855 (m), 2730 (w), 1642 (s), 1629 (s), 1595 (s), 1560 (m), 1539 (s), 1498 (s), 1489 (s), 1477 (s), 1441 (s), 1425 (s), 1407 (s), 1366 (s), 1327 (s), 1300 (m), 1219 (s), 1205 (s), 1189 (s), 1155 (m), 1145 (m), 1130 (w), 1090 (m), 1078 (m), 1055 (w), 1030 (w), 1012 (w), 967 (w), 957 (w), 947 (w), 898 (w), 874 (m), 854 (s), 831 (w), 824 (w), 778 (s), 746 (s), 693 (s), 669 (w), 635 (w), 604 (w), 578 (w), 546 (w), 513 (w), 484 (w), 431 (w) cm^{-1}. Anal. Calcd (found) for $C_{44}H_{40}N_4O$: C, 82.47 (82.58); H, 6.29 (6.59); N, 8.74 (8.33). Crystallization of the above sample from hexanes−acetone mixtures afforded the adduct $^{\text{Ph,Mes}}L_{DBF}H_2$·acetone (34.7%). IR: 3344 (s, br), 3059 (w), 3035 (w), 3024 (w), 2912 (m), 2854 (m), 1926 (w), 1694 (s, $\upsilon_{C=O}$), 1640 (s), 1595 (s), 1540 (s), 1499 (s), 1478 (s), 1442 (s), 1420 (s), 1404 (s), 1366 (m), 1357 (m), 1328 (s), 1260 (w), 1227 (s), 1206 (s), 1189 (s), 1128 (m), 1089 (w), 1076 (w), 1052 (w), 1030 (w), 1011 (w), 965 (w), 947 (w), 935 (w), 914 (w), 890 (w), 874 (w), 855 (m), 780 (m), 747 (s), 711 (w), 687 (m), 669 (w), 665 (w), 575 (w), 542 (w), 505 (w), 495 (w), 443 (w), 429 (w) cm^{-1}. Anal. Calcd (found) for $C_{47}H_{46}N_4O_2$: C, 80.77 (80.86); H, 6.63 (6.76); N, 8.02 (7.81).

$^{i\text{Pr}}$L$_{\text{Xan}}$H$_2$ was prepared from 9,9-dimethylxanthene and 1,3-diisopropylcarbodiimide by method A in 61% yield. ^{1}H NMR (C_6D_6): δ 7.13 (d, J = 7.6 Hz, 2H), 6.98 (d, J = 7.6 Hz, 2H), 6.88 (t, J = 7.6 Hz, 2H), 4.45 (br s, 2H, NC*H*Me$_2$), 3.50 (s, 2H, N*H*), 3.24 (br s, 2H, NC*H*Me$_2$), 1.44 (s, 6H, CMe_2), 1.23 (br s, 24H, CHMe_2) ppm. ^{13}C{^{1}H} NMR (C_6D_6): δ 152.1, 147.6, 130.9, 126.5, 126.0, 123.6, 51.3 (br), 42.8 (br), 34.8, 32.8 (br), 26.3 (br), 23.3 (br) ppm. One resonance in the ^{13}C{^{1}H} NMR spectrum is likely obscured by the solvent. IR (mineral oil mull): 3440 (m), 1639 (vs), 1488 (s), 1457 (s), 1426 (vs), 1374 (s), 1364 (m), 1322 (m), 1291 (m), 1279 (m), 1245 (s), 1200 (w), 1176 (m), 1121 (w), 1069 (w), 968 (w), 936 (w), 884 (m), 791 (m), 746 (s) cm^{-1}. Anal. Calcd (found) for $C_{29}H_{42}N_4O$: C, 75.28 (75.58); H, 9.15 (9.14); N, 12.11 (12.10).

$^{t\text{Bu,Et}}$L$_{\text{Xan}}$H$_2$ was prepared from 9,9-dimethylxanthene and 1-*tert*-butyl-3-ethylcarbodiimide by method A in 62.1% yield. ^{1}H NMR (C_6D_6): δ 7.12 (d, J = 7.2 Hz, 2H), 7.03 (d, J = 7.2 Hz, 2H), 6.90 (t, J = 7.6 Hz, 2H), 3.53 (m, 2H, NCH_2CH$_3$), 3.14 (m, 2H, NCH_2-CH$_3$), 1.55 (s, 18H, NCMe_3), 1.47 (s, 6H, CMe_2), 1.35 (t, J = 5.2 Hz, 6H, NCH$_2$CH_3) ppm. ^{13}C{^{1}H} NMR (C_6D_6): δ 152.6, 147.1, 130.3, 127.0, 126.7, 123.8, 52.0, 46.2, 34.6, 33.5, 29.8, 18.4 ppm. One resonance in the ^{13}C{^{1}H} NMR spectrum is likely obscured by the solvent. IR: 3441 (s), 3431 (s), 3286 (m), 3065 (m), 2965 (s), 2956 (s), 2927 (s), 2913 (s), 2862 (s), 2682 (w), 1931 (w), 1656 (s), 1650 (s), 1643 (s), 1598 (m), 1580 (m), 1560 (m), 1491 (s), 1460 (s), 1448 (s), 1428 (s), 1386 (s), 1369 (s), 1360 (s), 1356 (s), 1312 (s), 1297 (s), 1286 (s), 1251 (s), 1222 (s), 1170 (s), 1153 (m), 1133 (m), 1122 (m), 1100 (s), 1073 (s), 1058 (s), 1032 (m), 981 (w), 967 (w), 938 (w), 921 (m), 911 (w), 886 (s), 860 (m), 824 (w), 809 (s), 802 (m), 760 (s), 744 (s), 705 (m), 664 (w), 623 (w), 616 (w), 575 (w), 540 (w), 529 (w), 497 (w), 474 (w), 442 (w), 415 (w) cm^{-1}.

$^{i\text{Pr}}$L$_{\text{DBF}}$Al$_2$Me$_4$ (3). To a toluene (300 mL) solution of $^{i\text{Pr}}L_{DBF}H_2$ (10.0 g, 23.8 mmol) was added Al_2Me_6 (4.8 mL, 24.2 mmol). Gas evolution was observed, and the resulting white suspension was stirred at ambient temperature overnight. Removal of the volatile materials afforded a white solid, which was crystallized from Et_2O to give a colorless crystalline solid (5.28 g, 41.8%). ^{1}H NMR (C_6D_6): δ 7.51$_X$ (2H), 7.00$_B$ (2H), 6.99$_A$ (2H) (J_{BX} = 1.0 Hz, J_{AX} = 8.0 Hz, J_{AB} = 7.5 Hz), 3.15 (sept, J = 6.0 Hz, 4H, NC*H*Me$_2$), 1.03 (d, J = 6.0 Hz, 12H, NCHMe_2), 1.00 (d, J = 6.4 Hz, 12H, NCHMe_2), −0.01 (s, 6H, AlMe_2), −0.05 (s, 6H, AlMe_2) ppm. ^{13}C{^{1}H} NMR (C_6D_6): δ 168.8, 153.0, 127.6, 125.1, 123.9, 122.5, 116.0, 46.7, 25.9, 25.9, −8.9 (br, AlMe_2) ppm. IR: 3066 (m), 2965 (s), 2924 (s), 2868 (s), 2816 (m), 2723 (w), 2713 (w), 2611 (w), 2024 (w), 1939 (w), 1927 (w), 1882 (w), 1870 (w), 1583 (m), 1560 (w), 1482 (s, br), 1420 (s), 1404 (s), 1380 (s), 1363 (s), 1344 (s), 1338 (s), 1320 (s), 1273 (s), 1236 (w), 1228 (w), 1187 (s, br), 1125 (s), 1058 (s), 1030 (m), 971 (w), 964 (w), 957 (w), 941 (w), 922 (m), 861 (s), 836 (w), 793 (s), 755 (s), 728 (s, br), 674 (s, br), 590 (s), 569 (m), 508 (w), 420 (w), 413 (w) cm^{-1}. Anal. Calcd (found) for $C_{30}H_{46}N_4OAl_2$: C, 67.64 (67.34); H, 8.70 (8.93); N, 10.52 (10.20).

$^{i\text{Pr}}$L$_{\text{Xan}}$Al$_2$Me$_4$ (4). The synthesis was carried out analogously to that of **3**. The crude product was crystallized from ether to give a white crystalline solid in 75.0% yield. ^{1}H NMR (C_6D_6): δ 7.05 (d, J = 7.0 Hz, 2H), 6.83−6.78 (4H), 3.27 (sept, J = 6.5 Hz, 4H, NC*H*Me$_2$), 1.30 (s, 6H, CMe_2), 1.12 (d, J = 7.0 Hz, 12H, NCHMe_2), 0.98 (d, J = 6.0, 12H, NCHMe_2), 0.02 (s, 6H, AlMe_2), −0.11 (s, 6H, AlMe_2) ppm. ^{13}C{^{1}H} NMR (C_6D_6): δ 171.4, 147.1, 131.0, 129.1, 128.7, 124.0, 120.4, 46.6, 34.5, 33.4, 26.4, 25.7, −7.7 (br, AlMe_2), −8.4 (br, AlMe_2) ppm. IR: 3438 (w), 2962 (s), 2926 (s), 2868 (s), 2612 (w), 1637 (s, br), 1560 (w), 1467 (s, br), 1424 (s), 1381 (s), 1362 (s), 1340 (s), 1274 (m), 1241 (s), 1202 (m), 1179 (s), 1169 (s), 1122 (m), 1084 (w), 1055 (w), 961 (w), 930 (w), 916 (w), 910 (w), 880 (m), 826 (m), 801 (s), 753 (s), 741 (s), 709 (s, br), 673 (s), 592 (m), 522 (w), 459 (w), 439 (w), 419 (w) cm^{-1}. Anal. Calcd (found) for $C_{33}H_{52}N_4OAl_2$: C, 68.96 (68.79); H, 9.12 (9.35); N, 9.75 (9.62).

Table 1. Crystallographic Data and Collection Parameters

compound	$^{i\mathrm{Pr}}L_{\mathrm{DBF}}H_2\cdot Et_2O$	$^{\mathrm{Ph,Mes}}L_{\mathrm{DBF}}H_2\cdot$acetone	**3**	**4**
formula	$C_{30}H_{46}N_4O_2$	$C_{47}H_{46}N_4O_2$	$C_{30}H_{46}Al_2N_4O$	$C_{33}H_{52}Al_2N_4O$
formula wt	494.71	698.88	532.67	574.75
space group	*C*2/*c* (No. 15)	$P\bar{1}$ (No. 2)	$P\bar{1}$ (No. 2)	*C*2/*c* (No. 15)
temp (°C)	−138	−133	−129	−137
a (Å)	18.874(4)	10.871(1)	10.8509(4)	21.147(1)
b (Å)	8.630(2)	14.068(1)	12.2178(4)	11.5004(7)
c (Å)	19.207(4)	14.188(1)	14.1196(5)	29.858(2)
V (Å^3)	2958(1)	1910.8(3)	1658.6(1)	7202.6(7)
α (deg)	90	106.247(2)	72.503(1)	90
β (deg)	109.01(3)	92.611(3)	82.427(1)	97.293(1)
γ (deg)	90	111.536(2)	68.324(1)	90
Z	4	2	2	8
d_{calc} (g/cm^3)	1.111	1.215	1.067	1.060
θ range (deg)	2.24−25.03	2.04−23.26	1.51−27.48	2.02−24.99
μ (mm^{-1})	0.070	0.075	0.11	0.11
crystal dimensions (mm)	0.3 × 0.2 × 0.2	0.4 × 0.2 × 0.1	0.1 × 0.3 × 0.3	0.3 × 0.2 × 0.2
reflections collected	8 989	10 965	16 568	22 164
data/restraints/parameters	2620/−/169	5478/−/494	7606/0/346	6342/0/375
R1 (for $F_o > 4\sigma F_o$)	0.0592 (for 1735 data)	0.0614 (for 2998 data)	0.0643	0.0448
R1, wR2 (all data)	0.0910, 0.1770	0.1197, 0.1719	0.0841, 0.1904	0.0662, 0.1202
GOF	1.038	0.923	1.022	1.032
largest peak, hole (e/Å^3)	0.39, −0.37	0.37, −0.21	0.56, −0.31	0.22, −0.23

$^{t\mathrm{Bu,Et}}L_{\mathrm{DBF}}Al_2Me_4$ (5). The synthesis was carried out analogously to that of **3**. The crude product was crystallized from hexanes to give a white solid in 64.1% yield. ^{1}H NMR spectroscopy revealed the product to be a 1.0:0.98 mixture of rotational diastereomers with C_2 and C_s symmetry. We have not determined which set of resonances corresponds to each diastereomer. *Product A:* ^{1}H NMR (C_6D_6): *δ* 7.47−7.44 (2H), 6.99−6.92 (4H), 2.63 (sept, *J* = 6.0 Hz, 4H, NC*H*$_2$CH$_3$), 1.06 (s, 18H, NC*Me*$_3$), 0.94 (t, *J* = 7.5 Hz, 6H, NCH$_2$C*H*$_3$), 0.04 (s, 6H, Al*Me*$_2$), −0.05 (s, 6H, Al*Me*$_2$) ppm. ^{13}C{^{1}H} NMR (C_6D_6): *δ* 170.0, 152.6, 127.61, 124.8, 123.6, 122.2, 118.9, 52.0, 39.8, 32.3, 17.4, −9.22 (br, Al*Me*$_2$). *Product B:* ^{1}H NMR (C_6D_6): *δ* 7.47−7.44 (2H), 6.99−6.92 (4H), 2.64 (sept, *J* = 7.0 Hz, 4H, NC*H*$_2$CH$_3$), 1.07 (s, 18H, NC*Me*$_3$), 0.94 (t, *J* = 7.0 Hz, 6H, NCH$_2$C*H*$_3$), 0.04 (s, 6H, Al*Me*$_2$), −0.05 (s, 6H, Al*Me*$_2$) ppm. ^{13}C{^{1}H} NMR (C_6D_6): *δ* 169.9, 152.8, 127.8, 124.8, 123.5, 122.3, 118.8, 52.0, 39.8, 32.5, 17.4, −9.12 (br, Al*Me*$_2$). IR (mixture of A + B): 3438 (w), 3065 (w), 2967 (s), 2930 (s), 2887 (s), 2868 (s), 1648 (m, br), 1481 (s, br), 1459 (s), 1446 (s), 1422 (s), 1406 (s), 1390 (m), 1376 (s), 1362 (s), 1348 (s), 1276 (s), 1225 (m), 1186 (s, br), 1068 (m), 1031 (w), 919 (m), 863 (m), 790 (s), 757 (s), 731 (s), 673 (s), 619 (m), 581 (w), 473 (w) cm^{-1}.

$^{t\mathrm{Bu,Et}}L_{\mathrm{Xan}}Al_2Me_4$ (6). The synthesis was carried out analogously to that of **3**. The crude product was crystallized from hexanes to give a white solid in 57.6% yield. ^{1}H NMR spectroscopy revealed the product to be a 1.00:0.91 mixture of rotational diastereomers with C_2 and C_s symmetry, respectively. C_2-**6**: ^{1}H NMR (C_6D_6): *δ* 7.04 (d, *J* = 7.6 Hz, 2H), 6.84−6.74 (4H), 2.97−2.85 (2H, NC*H*CH$_3$), 2.74−2.61 (2H, NC*H*CH$_3$), 1.32 (s, 6H, C*Me*$_2$), 1.15 (s, 18H, NC*Me*$_3$), 1.01 (t, *J* = 7.2 Hz, 6H, NCH$_2$C*H*$_3$), 0.02 (s, 6H, Al*Me*$_2$), −0.11 (s, 6H, Al*Me*$_2$) ppm. ^{13}C{^{1}H} NMR (C_6D_6): *δ* 171.9, 146.5, 130.5, 129.2, 127.5, 123.7, 122.5, 52.0, 40.1, 34.4, 33.7, 32.3, 17.1, −7.6 (br, Al*Me*$_2$), −9.1 (br, Al*Me*$_2$) ppm. C_s-**6**: ^{1}H NMR (C_6D_6): *δ* 7.05 (d, *J* = 7.6 Hz, 2H), 6.84−6.74 (4H), 2.97−2.85 (2H, NC(H)*H*Me), 2.74−2.61 (2H, NC*H*CH$_3$), 1.42 (s, 3H, C*Me*$_2$), 1.19 (s, 3H, C*Me*$_2$), 1.16 (s, 18H, NC*Me*$_3$), 0.97 (t, *J* = 7.2 Hz, 6H, NCH$_2$C*H*$_3$), 0.01 (s, 6H, Al*Me*$_2$), −0.11 (s, 6H, Al*Me*$_2$) ppm. ^{13}C{^{1}H} NMR (C_6D_6): *δ* 171.7, 147.2, 131.0, 129.1, 128.1, 123.7, 122.4, 51.9, 39.9, 35.7, 34.6, 32.5, 29.4, 17.1, −7.6 (br, Al*Me*$_2$), −9.1 (Al*Me*$_2$) ppm. IR (C_2-**6** and C_s-**6** mixture): 3440 (w), 3068 (m), 2965 (s), 2928 (s), 2885 (s), 2868 (s), 2818 (m), 1648 (s), 1624 (s), 1596 (m), 1582 (m), 1499 (s), 1479 (s), 1458 (s), 1444 (s), 1427 (s), 1390 (s), 1375 (s), 1364 (s), 1348 (s), 1276 (s), 1250 (s), 1235 (s), 1185 (s), 1109 (m), 1077 (w), 1065 (w), 1032 (w), 1009 (w), 954 (m), 913 (w), 884 (m), 827 (m), 804 (s), 789 (s), 750 (w), 714 (s), 671 (s), 617 (m), 578 (m), 479 (w), 422 (w) cm^{-1}.

Table 2. Selected Bond Distances and Angles

$^{i\mathrm{Pr}}L_{\mathrm{DBF}}H_2$		**3**	
N1−C4	1.382(3)	Al1−N1	1.942(2)
N1−C2	1.454(3)	Al1−N2	1.928(2)
N2−C4	1.280(3)	Al1−C27	1.955(2)
N2−C12	1.462(3)	Al1−C28	1.954(2)
C2−N1−C4	124.3(2)	Al2−N3	1.936(2)
C4−N2−C12	119.4(2)	Al2−N4	1.937(2)
N1−C4−C5	110.7(2)	Al2−C29	1.951(2)
N1−C4−N2	121.2(2)	Al2−C30	1.953(2)
N2−C4−C5	128.0(2)	Al1−Al2	6.5050(9)
		N1−Al1−N2	68.94(7)
		C27−Al1−C28	116.7(1)
		N3−Al2−N4	69.05(7)
		C29−Al2−C30	119.7(1)
$^{\mathrm{Ph,Mes}}L_{\mathrm{DBF}}H_2\cdot$acetone		**4**	
O2−N2	3.026(4)	Al1−N1	1.923(2)
O2−N3	2.990(4)	Al1−N2	1.947(2)
O2−H1	2.19(4)	Al1−C30	1.956(3)
O2−H2	2.17(4)	Al1−C31	1.948(2)
N2−H1	0.87(4)	Al2−N3	1.930(2)
N3−H2	0.85(4)	Al2−N4	1.934(2)
N1−C16	1.291(4)	Al2−C32	1.949(2)
N2−C16	1.364(5)	Al2−C33	1.955(2)
N4−C29	1.282(4)	Al1−Al2	5.9303(9)
N3−C29	1.367(4)	N1−Al1−N2	68.83(7)
O2−C46	1.206(4)	C30−Al1−C31	116.7(1)
N2−H2−O2	161(3)	N3−Al2−N4	69.17(9)
N3−H2−O2	163(3)	C32−Al2−C33	117.2(1)
H1−O2−H2	97(1)		
C46−O2−H1	132(1)		
C46−O2−H2	120(1)		

X-ray Crystallography. Table 1 lists a summary of crystal data and collection parameters for all crystallographically characterized compounds. Single-crystal structure determinations were performed within the Department of Chemistry and Biochemistry at the University of Colorado.

General Procedure. A crystal of appropriate size was mounted on a glass fiber using Paratone-N oil, transferred to a Siemens SMART diffractometer/CCD area detector, centered in the beam

(Mo Kα; $\lambda = 0.710\ 73$ Å; graphite monochromator), and cooled to −130(5) °C by a nitrogen low-temperature apparatus. Preliminary orientation matrix and cell constants were determined by collection of 60 10-s frames, followed by spot integration and least-squares refinement. A sphere of data was collected using 0.3° ω scans. The raw data were integrated and the unit cell parameters refined using SAINT. Data analysis was performed using XPREP. Absorption correction was applied using SADABS. The data were corrected for Lorentz and polarization effects, but no correction for crystal decay was applied. Structure solutions and refinements were performed (SHELXTL-Plus V5.0) on *F*-squared.

X-ray Diffraction Study of $^{i\mathrm{Pr}}\mathrm{L_{DBF}H_2}\cdot\mathrm{Et_2O}$. Crystals suitable for X-ray diffraction studies were grown from Et_2O at −40 °C. Preliminary data indicated a C-centered monoclinic cell. Analysis of all data indicated systematic absences which were consistent with space groups *C*2/*c* (No. 15) and *Cc* (No. 9). The choice of *C*2/*c* was confirmed by the successful solution and refinement of the structure. The molecule rests on a crystallographic C_2-axis that passes through O(1). All non-H atoms were refined anisotropically. H(1) was located in a difference Fourier map and was refined isotropically. All other H-atoms were placed in idealized positions and were included in structure factor calculations but were not refined. The asymmetric unit also contains one-half molecule of cocrystallized Et_2O, roughly located on a crystallographic inversion center.

X-ray Diffraction Study of $^{\mathrm{Ph,Mes}}\mathrm{L_{DBF}H_2}\cdot$Acetone. Crystals suitable for X-ray diffraction studies were grown from a 1% acetone in hexanes mixture at room temperature. Preliminary data indicated a triclinic cell. The choice of the centric cell was confirmed by the successful solution and refinement of the structure. All non-H atoms were refined anisotropically. The amidine H-atoms, H(1) and H(2), were located in a difference Fourier map and were refined isotropically. All other H-atoms were placed in idealized positions and were included in structure factor calculations but were not refined.

X-ray Diffraction Study of 3. Crystals suitable for X-ray diffraction studies were grown from Et_2O at −40 °C. Preliminary data indicated a triclinic cell. The choice of the centric cell was confirmed by the successful solution and refinement of the structure. All non-H atoms were refined anisotropically. Hydrogens were placed in idealized positions and were included in structure factor calculations but were not refined.

X-ray Diffraction Study of 4. Crystals suitable for X-ray diffraction studies were grown from Et_2O at −40 °C. Preliminary data indicated a C-centered monoclinic cell. Systematic absences were consistent with space groups *C*2/*c* (No. 15) and *Cc* (No. 9). The choice of former was confirmed by the successful solution and refinement of the structure. All non-H atoms were refined anisotropically. Hydrogens were placed in idealized positions and were included in structure factor calculations but were not refined.

NMR Studies. NMR experiments were performed on Varian Inova 500 and Inova 400 NMR spectrometers, operating at 500.1 and 400.15 MHz, respectively, for proton observation. Dynamic exchange experiments (1D GOESY) were performed at 400.15 MHz, using frequency-shifted, shaped-selective pulses with a bandwidth of 15 Hz, centered on one of the Al−Me resonances. Mixing times of 0.1, 0.2, 0.4, 0.8, 1.5, and 2.5 s were used. To determine exchange rate constants, the intensity of the exchange peak (I_{exch}) is divided by the selected peak intensity (I_{sel}), and this ratio is plotted vs mixing time. The data are fit to the 2D-EXCHSY equation $I_{\mathrm{exch}}/I_{\mathrm{sel}} = [1 - \exp(-KT_{\mathrm{mix}})]/[1 + \exp(-KT_{\mathrm{mix}})]$ using nonlinear least squares curve fitting, yielding the exchange rate constant *K*.

Acknowledgment. We thank the Petroleum Research Fund (38046-G3), administered by the American Chemical Society, and the University of Colorado for financial support. NMR instrumentation used in this work was supported in part by the National Science Foundation CRIF program (CHE-0131003).

Supporting Information Available: Full details of crystallographic studies of $^{i\mathrm{Pr}}\mathrm{L_{DBF}H_2}\cdot\mathrm{Et_2O}$, $^{i\mathrm{Pr}}\mathrm{L_{Xan}H_2}$, $^{\mathrm{Ph,Mes}}\mathrm{L_{DBF}H_2}\cdot$acetone, **3**, and **4** are presented in Crystallographic Information File (CIF) format. This material is available free of charge via the Internet at http://pubs.acs.org.

IC035035P